PROCEEDINGS OF THE
AMERICAN MATHEMATICAL SOCIETY
Volume 150, Number 4, April 2022, Pages 1749–1765
https://doi.org/10.1090/proc/15750
Article electronically published on January 20, 2022

UNIQUENESS OF CLIFFORD TORUS WITH PRESCRIBED ISOPERIMETRIC RATIO

THOMAS YU AND JINGMIN CHEN

(Communicated by Jiaping Wang)

Abstract. The Marques-Neves theorem asserts that among all the torodial (i.e. genus 1) closed surfaces, the Clifford torus has the minimal Willmore energy $\int H^2\, dA$. Since the Willmore energy is invariant under Möbius transformations, it can be shown that there is a one-parameter family, up to homotheties, of genus 1 Willmore minimizers. It is then a natural conjecture that such a minimizer is unique if one prescribes its isoperimetric ratio. In this article, we show that this conjecture can be reduced to the positivity question of a polynomial recurrence. A proof of the positivity can be found in the companion article by Melczer and Mezzarobba [submitted to J. Comb. Theory (2020)]. This establishes a first uniqueness result for the Canham model of biomembranes.

1. Introduction

In this paper, we provide the proof, modulo a final step to be presented in the article [13], of the following result:

Theorem 1.1. *The 3-D Euclidean shape of the Clifford torus*

$$\{[\cos u, \sin u, \cos v, \sin v]^T/\sqrt{2} : u, v \in [0, 2\pi]\}$$

in $\mathbb{S}^3$ stereographically projected to $\mathbb{R}^3$ is uniquely determined by its isoperimetric ratio.

In above, two subsets of $\mathbb{R}^3$ have the same Euclidean shape if they can be transformed from one to another by a homothety. The isoperimetric ratio of a closed orientable surface is defined by $v := \mathrm{Vol}/[(4\pi/3)(\mathrm{Area}/4\pi)^{3/2}]$.

For an account of the interest of this result in connection to the Marques-Neves theorem [10] and the uniqueness of solution of the Canham-Evans-Helfrich model for biomembranes, see [16, Page 1-4] and the article [9] in the Spring 2016 MSRI newsletter. This result also furnishes a rigorous test case for the study of numerical methods; see [4] and the references therein.

Let $T_R := \{(R + \cos v) \cos u, (R + \cos v) \sin u, \sin v) : u, v \in [0, 2\pi]\}$, a torus embedded in 3-space with major radius $R \in (1, \infty)$, minor radius 1. Let $i_{(x,y,z)}$ be the inversion map about the unit sphere centered at (x, y, z) of $\mathbb{R}^3$. Recall that the set

Received by the editors November 19, 2020, and, in revised form, July 19, 2021.
2020 *Mathematics Subject Classification.* Primary 53A05, 53Z10, 33C99.
Key words and phrases. Canham-Evans-Helfrich model, Willmore energy, Clifford torus, Möbius geometry, Marques-Neves theorem, uniqueness, P-recurrence, special functions, positivity.
The first author was supported in part by the National Science Foundation grants DMS 0512673 and DMS 0915068. This work was partially supported by NSF grants DMS 0915068 and DMS 1115915.

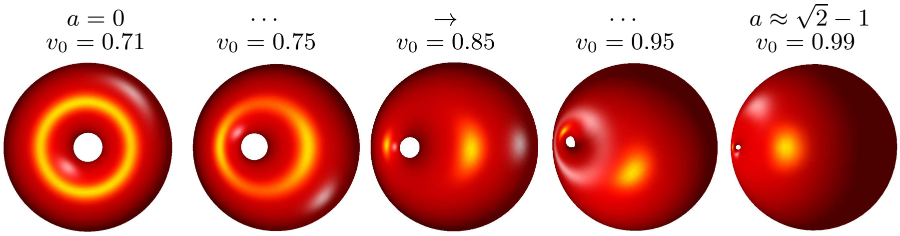

FIGURE 1. $i_{(a,0,0)}(T_{\sqrt{2}})$ as a increases from 0 to $\sqrt{2}-1$. By Theorem 2.4, these are all the possible non-homothetic images of $T_{\sqrt{2}}$ under Möb(3). By Pappus's theorems, the isoperimetric ratio of the surface of revolution Clifford torus $T_{\sqrt{2}}$ is $(3/2)(2\pi^2)^{-1/4} \approx 0.71$.

of all stereographic images of the Clifford torus in $\mathbb{S}^3$ to $\mathbb{R}^3$ is tantamount to the set of all images of $T_{\sqrt{2}}$ under Möb(3), the 3-D Möbius group consisting of all rigid motions, scaling, and sphere inversions.

The proof of Theorem 1.1 connects ideas in geometry and combinatorics and is divided into four steps:

I. Prove that the set of all non-homethetic images of $T_{\sqrt{2}}$ under Möb(3) corresponds exactly to the one-parameter family

$$\{i_{(a,0,0)}(T_{\sqrt{2}}) : a \in [0, \sqrt{2}-1)\}. \tag{1.1}$$

In other words, the cyclides depicted in Figure 1 are exactly the set of all non-homothetic Clifford tori. This is established in Theorem 2.4 of Section 2.[1]

II. With this result, the conjecture follows if we can show:

$$\mathrm{Iso} : [0, \sqrt{2}-1) \to [(3/2)(2\pi^2)^{-1/4}, 1), \quad \mathrm{Iso}(a) := v\big(i_{(a,0,0)}(T_{\sqrt{2}})\big) \tag{1.2}$$

is a bijection. If so, then each $v_0 \in [(3/2)(2\pi^2)^{-1/4}, 1)$ corresponds to one and only one Clifford torus, namely $i_{(\mathrm{Iso}^{-1}(v_0),0,0)}(T_{\sqrt{2}})$, with isoperimetric ratio v_0, which must be the unique solution of the genus 1 Canham problem with v_0 as the constrained isoperimetric ratio.

To prove that Iso is a bijection, it suffices to show that Iso is monotonic increasing and

$$\lim_{a \to \sqrt{2}-1} \mathrm{Iso}(a) = 1. \tag{1.3}$$

In Section 3, we establish Theorem 3.1, which is a more general version of (1.3).

[1]While $\dim \text{Möb}(3) = 10$, the fact that there is only one degree of freedom in the set of all non-homethetic images of $T_{\sqrt{2}}$ under Möb(3) should be quite trivial to those versed in the subject: the 7-dimensional subgroup of Möb(3) consisting of the homotheties in $\mathbb{R}^3$, by definition, contributes nothing to the Euclidean shapes. Next, a subgroup of $SO(4)$ isomorphic to $SO(1) \times SO(1)$ clearly leaves the Clifford torus in $\mathbb{S}^3$ invariant; this takes away two more degrees of freedom. (The 2-parameter family of congruent transformations in Möbius geometry are neither congruences nor similarities in Euclidean geometry.) The explicit one-to-one correspondence between the inversion parameter 'a' and the 'shape space' requires a more prudent effort.

III. To prove that Iso is monotonic increasing, we venture into the realm of special functions. We make the observation that the area and enclosed volume of the cyclides in (1.1), denoted by $A(a)$ and $V(a)$, can be extended analytically to the disc $\{z : |z| < \sqrt{2}-1\}$ on the complex plane. Moreover, the coefficients $(a_n)_{n\geqslant 0}$ and $(v_n)_{n\geqslant 0}$ of their power series at $z = 0$ are holonomic, or P-recursive, sequences, i.e. they satisfy linear recurrences with polynomial coefficients. We work out explicitly these P-recurrences in Section 4.

Since $\mathrm{Iso}^2(a)/(36\pi) = V^2(a)/A^3(a)$, Iso is monotonic increasing iff the logarithm of the right-hand side is. But then we have

$$\frac{d}{da}\ln\frac{V^2(a)}{A^3(a)} = \frac{2V'(a)A(a) - 3V(a)A'(a)}{V(a)A(a)},$$

so Iso is monotonic increasing iff $2V'(a)A(a) - 3V(a)A'(a) > 0$ on $[0, \sqrt{2}-1)$. The fact that $A(z)$ and $V(z)$ are holonomic implies that $D(z) := 2V'(z)A(z) - 3V(z)A'(z)$ is also holonomic; the coefficient $(d_n)_{n\geqslant 0}$ of the power series of $D(z)$ at $z = 0$ follows the P-recurrence (4.7) derived in Section 4.

The monotonicity of Iso follows if all the terms defined by the P-recurrence (4.7) are positive.

*IV. Prove that all terms defined by the P-recurrence (4.7) are positive.

This last step is carried out in [13].

Steps I–III are carried out in the next three sections.

2. Step I: Non-homothetic Clifford tori

Our first goal is to characterize all the Euclidean shapes of the Clifford tori, i.e. we would like to find a parametrization of the 'shape space'

$$\left\{ i_{(x,y,z)}(T_{\sqrt{2}}) : (x,y,z) \in \mathbb{R}^3 \backslash T_{\sqrt{2}} \right\} \Big/ \mathrm{Hom}(3). \tag{2.1}$$

Here '/Hom(3)' means we identify two point sets if they can be transformed from one to another by a homothety in $\mathbb{R}^3$. Since we are primarily interested in Euclidean shapes here, we avoid sphere inversions centered at points on T_R itself. To help us gain a better insight of the underlying structure, we also study the more general shape space

$$\left\{ i_{(x,y,z)}(T_R) : R > 1,\ (x,y,z) \in \mathbb{R}^3 \backslash T_R \right\} \Big/ \mathrm{Hom}(3). \tag{2.2}$$

Maxwell's characterization of a cyclide. It is well-known that any (torodial) cyclide $\mathfrak{C}$ has two orthogonal planes of mirror symmetry; see, for example, [2,3,11]. We make the observation that the Euclidean shape of a toroidal cyclide $\mathfrak{C}$ is uniquely determined by certain measurements of the cross section of $\mathfrak{C}$ with either one of the two symmetry planes.

We use Maxwell's characterization of cyclides [2,3,11]: any cyclide $\mathfrak{C}$ is the envelope of all the spheres centered at the points P on a given ellipse $\mathcal{E}$ with radii $r(P)$, $P \in \mathcal{E}$, satisfying $r(P) + \overline{FP} = L$, where F is one of the foci of $\mathcal{E}$ and L is a constant in a suitable range. We can think of L as the length of a taut string attached in one end to F; the string slides smoothly on $\mathcal{E}$ and traces out spheres with the other end. See Figure 2. Under this characterization, $\mathfrak{C}$ is a torodial cyclide if and only if

$$a > L - a > f,$$

where a, f and L are the major radius of $\mathcal{E}$, the focal length of $\mathcal{E}$, and the length of the string, respectively. Moreover, the Euclidean shape of $\mathfrak{C}$ can be characterized by the ratio $a : f : L$.[2]

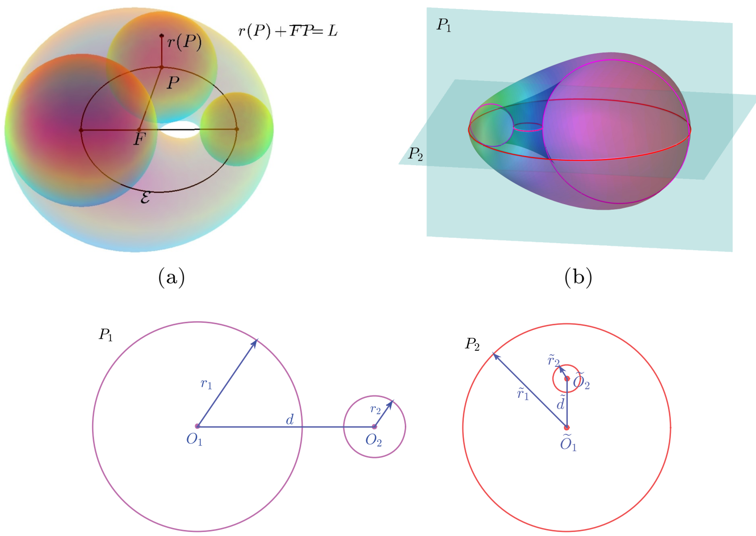

(a) (b)

(c) $i_{(x,y,z)}(T_R) \cap P_1$ (d) $i_{(x,y,z)}(T_R) \cap P_2$

FIGURE 2. (a) Maxwell's characterization of a torodial cyclide. (b) Two planes of mirror symmetry. (c) and (d) Cross sections of $i_{(x,y,z)}(T_R)$ with P_1 and P_2.

The major axis of $\mathcal{E}$ lies on the intersecting line of the two symmetry planes of $\mathfrak{C}$. In the following, P_1 refers to the symmetry plane where $\mathcal{E}$ lies, whereas P_2 ($\perp P_1$) refers to the other symmetry plane. The cross section $\mathfrak{C} \cap P_1$ consists of two circles **exterior to each other**, whereas the cross section $\mathfrak{C} \cap P_2$ consists of two circles with **one lying inside the other** (see Figure 2).

Denote the radii of the two circles in $\mathfrak{C} \cap P_1$ by r_1 and r_2 and the distance between the two centers by d (see Figure 2). Similarly, let $\tilde{r}_1$ and $\tilde{r}_2$ be the radii of the two circles in $\mathfrak{C} \cap P_2$ and $\tilde{d}$ be the distance between the two centers. By convention, $r_1 \geqslant r_2$, $\tilde{r}_1 \geqslant \tilde{r}_2$. The three sets of measurements (r_1, r_2, d), $(\tilde{r}_1, \tilde{r}_2, \tilde{d})$ and (a, f, L) of a cyclide $\mathfrak{C}$ are related by the following equations:

$$a = \frac{d}{2}, \quad f = \frac{r_1 - r_2}{2}, \quad L = \frac{d + r_1 + r_2}{2}. \tag{2.3}$$

$$\tilde{r}_1 = \frac{d + (r_1 + r_2)}{2}, \quad \tilde{r}_2 = \frac{d - (r_1 + r_2)}{2}, \quad \tilde{d} = r_1 - r_2. \tag{2.4}$$

Since the maps $(a, f, L) \mapsto (r_1, r_2, d)$ and $(r_1, r_2, d) \mapsto (\tilde{r}_1, \tilde{r}_2, \tilde{d})$ are linear isomorphisms, we conclude that:

[2]This already explains why the shape space (2.2) is two-dimensional.

Lemma 2.1. *Each of the three ratios $a : f : L$, $r_1 : r_2 : d$ and $\tilde{r}_1 : \tilde{r}_2 : \tilde{d}$ determines the Euclidean shape of the cyclide $\mathfrak{C}$.*

For any $\varrho > 0$, let $\mathcal{C}(\varrho) = \mathcal{C}(\varrho; R)$ be the circle in the ϱ-z plane with a diameter connecting $(\varrho, 0)$ and $\big((R^2-1)/\varrho, 0\big)$; see Figure 3. By convention, $\mathcal{C}(0) = \mathcal{C}(\infty)$ is the z-axis. In general, we have

$$C(\varrho) = C((R^2-1)/\varrho).$$

These circles on the plane can be extended to the following tori in 3-D:

$$\mathcal{T}(\varrho) := \mathcal{T}(\varrho; R) := \{(\rho\cos(\theta), \rho\sin(\theta), z) : (\rho, z) \in \mathcal{C}(\varrho),\ \theta \in [0, 2\pi]\}. \tag{2.5}$$

For any fixed R, the torus $\mathcal{T}(\varrho)$ lies completely outside, on, or inside the torus T_R when $\varrho \in [0, R-1) \cup (R+1, \infty]$, $\varrho = R \mp 1$, or $\varrho \in (R-1, R+1)$, respectively. In particular, $\mathcal{T}(R \pm 1; R) = T_R$. On the ρ-z plane, these correspond to the red, green and blue circles in Figure 3(a). While the one-parameter family of circles $\big\{\mathcal{C}(\varrho) : \varrho \in [0, \sqrt{R^2-1}]\big\}$ partitions the ρ-z plane,[3] the corresponding one-parameter family of tori $\big\{\mathcal{T}(\varrho) : \varrho \in [0, \sqrt{R^2-1}]\big\}$ partitions $\mathbb{R}^3$. We shall see that how these circles and tori characterize the shape spaces (2.1) and (2.2).

Theorem 2.2. *For any fixed $R \in (1, \infty)$ and $\varrho \in [0, \infty]\backslash\{R-1, R+1\}$, all the cyclides in*

$$\Big\{ i_{(x,y,z)}(T_R) : \quad (x, y, z) \in \mathcal{T}(\varrho; R) \Big\}, \tag{2.6}$$

are homothetic in $\mathbb{R}^3$.

Proof. We divide the proof into 3 steps.

1° By rotational symmetry, the shape of $i_{(\rho\cos(\theta), \rho\sin(\theta), z)}(T_R)$ is independent of θ. So it suffices to prove that all cyclides of the form

$$i_{(\rho,0,z)}(T_R), \quad (\rho, z) \in \mathcal{C}(\varrho),$$

are homothetic.

By Lemma 2.1, the Euclidean shape of $i_{(\rho,0,z)}(T_R)$ is determined by the measurements of its cross section at the x-z plane. Denote by P the x-z plane and $\pi : \mathbb{R}^3 \to \mathbb{R}^2$ be the ortho-projection map onto P. Note that

$$\pi\left(i_{(\rho,0,z)}(T_R) \cap P\right) = i_{(\rho,z)}\left(\pi(T_R \cap P)\right). \tag{2.7}$$

Here $i_{(\rho,z)}$ stands for the circle inversion map in 2-D with respect to the unit circle centered at (ρ, z). Note that P is a symmetry plane of the cyclides (2.7) and that the cross section (2.7) consists of a circle pair. Therefore, by (the implication of) Lemma 2.1, it suffices to check that these circle pairs corresponding to different $(\rho, z) \in \mathcal{C}(\varrho)$ are all homothetic. We have reduced the problem into one of plane geometry.

[3] Any (ρ, z), $\rho > 0$, lies on the circle $\mathcal{C}(\varrho^+) = \mathcal{C}(\varrho^-)$, where $\varrho^\pm = \frac{(\rho^2+z^2+R^2-1) \pm \sqrt{(\rho^2+z^2+R^2-1)^2 - 4\rho^2(R^2-1)}}{2\rho}$.

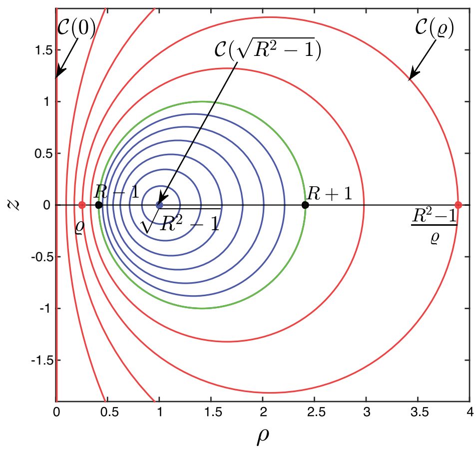

(a)

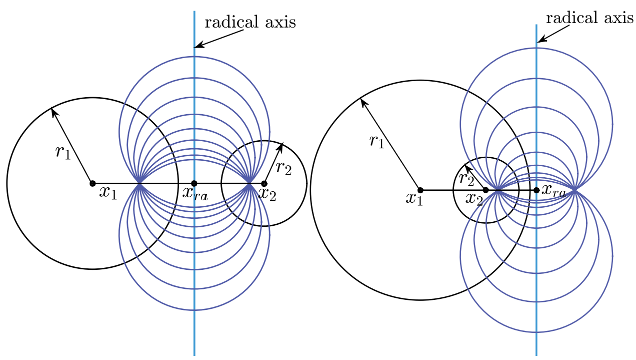

(b)

FIGURE 3. (a) $\mathcal{C}(\varrho)$ for various values of $\varrho \in (0, R-1)$ (in red) and $\varrho \in (R-1, \sqrt{R^2-1})$ (in blue). Note that $\mathcal{C}(\varrho) = \mathcal{C}((R^2-1)/\varrho)$ and $\mathcal{C}(\sqrt{R^2-1})$ degenerates into a point. (b) Radical axis of a circle pair: (left) two circles exterior to each other; (right) one circle lying inside the other. The blue circles meet the circle pair orthogonally.

2° We recall a well-known fact about circle inversion. If we invert two circles centered at $(x_1, 0)$ and $(x_2, 0)$ with radii r_1 and r_2 about a circle centered anywhere on the line

$$\left\{ (x_{ra}, y) \;\middle|\; x_{ra} = \frac{(x_2^2 - x_1^2) + (r_1^2 - r_2^2)}{2(x_2 - x_1)} \right\}, \tag{2.8}$$

the resulting circle pair is homothetic to the original circle pair. This line is called the *radical axis* of the circle pair; see Figure 3(b).

We first determine the image of the circle pair $\pi(T_R \cap P)$ under the circle inversion $i_{(\varrho,0)}$. The circle pairs in $\pi(T_R \cap P)$ consist of two unit circles with diameters A_1B_1 and A_2B_2, both on the x-axis, with $A_1 = (R-1, 0)$, $B_1 = (R+1, 0)$, $A_2 = (-(R+1), 0)$ and $B_2 = (-(R-1), 0)$. The images of A_1, B_1, A_2, B_2 under

$i_{(\varrho,0)}$, denoted by A_1', B_1', A_2', B_2', again lie on the x-axis and form the diameters $A_1'B_1'$, $A_2'B_2'$ of circle pair in $i_{(\varrho,0)}(\pi(T_R\cap P))$.

- When $\varrho\in(0,R-1)$, $B_2'<A_2'<B_1'<A_1'$.[4]
- When $\varrho\in(R+1,\infty)$, $B_1'<A_1'<B_2'<A_2'$.
- When $\varrho\in(R-1,R+1)$, $A_1'<B_2'<A_2'<B_1'$.

In the first two cases, the circle pair are exterior of each other, as in Figure 3(a); in the last case, one circle lies inside the other, as in Figure 3(b). In any case, the resulting circle pair has the following radii and centers:
(2.9)

$$\mathfrak{r}_1=\frac{|A_1'-B_1'|}{2}=\frac{1}{|(\varrho-R)^2-1|},\quad \mathfrak{r}_2=\frac{|A_2'-B_2'|}{2}=\frac{1}{(\varrho+R)^2-1}$$

$$O_1=\frac{A_1'+B_1'}{2}=\Big(\varrho-\frac{\varrho-R}{(\varrho-R)^2-1},0\Big),\quad O_2=\frac{A_2'+B_2'}{2}=\Big(\varrho-\frac{\varrho+R}{(\varrho+R)^2-1},0\Big).$$

By (2.8) and (2.9), the radical axis of the circle pair $i_{(\varrho,0)}(\pi(T_R\cap P))$ is given by $\{(\rho_{ra},z):z\in\mathbb{R}\}$ where

$$\rho_{ra}=\varrho-\frac{\varrho}{\varrho^2+1-R^2}.$$

Now the circle pairs in

$$\Big\{i_{(\rho_{ra},z)}\circ i_{(\varrho,0)}(\pi(T_R\cap P)):\ z\in\mathbb{R}\Big\} \tag{2.10}$$

are all homothetic. The theorem is proved if we show that every circle pair in $\Big\{i_{(\rho,z)}(\pi(T_R\cap P)):\ (\rho,z)\in\mathcal{C}(\varrho)\Big\}$ is homothetic to some circle pair in (2.10). We do so in the last step of the proof.

3° Since an arbitrary composition of inversions can be written as a composition of an inversion (of radius 1) with a homothety (see [1, Page 92]),

$$i_{(\rho_{ra},z)}\circ i_{(\varrho,0)}=\mathcal{H}\circ i_{(\rho_1,z_1)}. \tag{2.11}$$

We can determine (ρ_1,z_1) using the following properties of an inversion i_O to find (ϱ_1,z_1): $i_O(O)=\infty$, $i_O(\infty)=O$, and $i_O(Q_1)=Q_2\Leftrightarrow i(Q_2)=Q_1$. By the first property,

$$i_{(\rho_{ra},z)}\circ i_{(\varrho,0)}(\rho_1,z_1)=\mathcal{H}\circ i_{(\rho_1,z_1)}(\rho_1,z_1)=\infty.$$

By the second property,

$$i_{(\varrho,0)}(\rho_1,z_1)=(\rho_{ra},z).$$

By the third property,

$$(\rho_1,z_1)=i_{(\varrho,0)}(\rho_{ra},z).$$

This means the set of all (ρ_1,z_1) in (2.11) is the image of the line $\{(\rho_{ra},z)|z\in\mathbb{R}\}$ under the inversion $i_{(\varrho,0)}$, which is a circle. By symmetry, this circle has a diameter on the x-axis. One end of the diameter is $i_{(\varrho,0)}((\rho_{ra},\infty))=(\varrho,0)$, and the other end is $i_{(\varrho,0)}((\varrho_{ra},0))=\frac{R^2-1}{\varrho}$. The circle is $\mathcal{C}(\varrho)$. ∎

In virtue of Theorem 2.2, we use the shorthand notation

$$i_\varrho(T_R)$$

to represent the common Euclidean shape of the cyclides in (2.6). Formally, $i_\varrho(T_R)$ is an element in the shape space (2.2).

[4]Here and below, $A<B$ simply means A is on the left of B for two points A and B are on the first axis of $\mathbb{R}^2$.

To further analyze the shape $i_\varrho(T_R)$, by Lemma 2.1 and Theorem 2.2, it suffices to analyze the ratio $r_1 : r_2 : d$ of the cross-section of $i_{(\varrho,0,0)}(T_R)$ at its P_1 symmetry plane.

Lemma 2.3. *For any $R \in (1,\infty)$, the P_1 cross section of $\mathfrak{C} = i_{(\varrho,0,0)}(T_R)$ has the following measurements:*

(i) *when $\varrho \in [0, R-1)$ (corresponding to the red circles in Figure* 3(a)*), the P_1 symmetry plane of $\mathfrak{C}$ is the x-z plane, and*

(2.12)
$$r_1 : r_2 : d = \lambda : 1 : \sqrt{(\lambda-1)^2 + 4\lambda R^2}, \quad \textit{where } \lambda = \frac{r_1}{r_2} = \frac{(\varrho+R)^2-1}{(\varrho-R)^2-1} \in [1,\infty).$$

(ii) *when $\varrho \in \left(R-1, \sqrt{R^2-1}\right]$ (corresponding to the blue circles in Figure* 3(a)*), the P_1 symmetry plane of $\mathfrak{C}$ is the x-y plane, and*

$$r_1 : r_2 : d = \lambda : 1 : \sqrt{(\lambda-1)^2 + 4\lambda\frac{R^2}{R^2-1}}, \tag{2.13}$$
$$\textit{where } \lambda = \frac{r_1}{r_2} = \frac{(R-1)[(R+1)^2-\varrho^2]}{(R+1)[\varrho^2-(R-1)^2]} \in [1,\infty).$$

Proof. The first two steps of the proof of Theorem 2.2 imply that

$$P, \text{the } x\text{-}z \text{ plane, is } \begin{cases} \text{the } P_1 \text{ symmetry plane of } \mathfrak{C} \text{ when } \varrho \in [0, R-1) \\ \text{the } P_2 \text{ symmetry plane of } \mathfrak{C} \text{ when } \varrho \in \left(R-1, \sqrt{R^2-1}\right] \end{cases}.$$

In the first case, $\mathfrak{r}_i$ and O_i in (2.9) are such that $\mathfrak{r}_1 > \mathfrak{r}_2$ and $O_2 < O_1$, and they give the (r_1, r_2, d) measurements of $\mathfrak{C}$:

$$r_1 = \frac{1}{(\varrho-R)^2-1}, \quad r_2 = \frac{1}{(\varrho+R)^2-1}, \quad d = \frac{\varrho+R}{(\varrho+R)^2-1} - \frac{\varrho-R}{(\varrho-R)^2-1}. \tag{2.14}$$

In the second case, we also have $\mathfrak{r}_1 > \mathfrak{r}_2$ but now $O_1 < O_2$, and they give the $(\tilde{r}_1, \tilde{r}_2, \tilde{d})$ measurements of $\mathfrak{C}$:

$$\tilde{r}_1 = \frac{1}{1-(\varrho-R)^2}, \quad \tilde{r}_2 = \frac{1}{(\varrho+R)^2-1}, \quad \tilde{d} = -\frac{\varrho+R}{(\varrho+R)^2-1} + \frac{\varrho-R}{(\varrho-R)^2-1}.$$

By (2.4), we can convert the $(\tilde{r}_1, \tilde{r}_2, \tilde{d})$ measurements to the (r_1, r_2, d) measurements via $r_1 = (\tilde{r}_1 - \tilde{r}_2 + \tilde{d})/2$, $r_2 = (\tilde{r}_1 - \tilde{r}_2 - \tilde{d})/2$, $d = \tilde{r}_1 + \tilde{r}_2$, so

(2.15)
$$r_1 = \frac{R-1}{\varrho^2-(R-1)^2}, \quad r_2 = \frac{R+1}{(R+1)^2-\varrho^2}, \quad d = \frac{1}{(R+\varrho)^2-1} - \frac{1}{(R-\varrho)^2-1}.$$

By routine computations, (2.12) follows from (2.14) and (2.13) follows from (2.15). ∎

Lemma 2.3 has an almost immediate consequence:

Theorem 2.4. *For any $R \in (1,\infty)$, $i_\varrho(T_R)$ is distinct for each $\varrho \in [0, R-1)$.*

- *If $R \neq \sqrt{2}$, then $i_\varrho(T_R)$ is distinct for each $\varrho \in [0, R-1) \cup (R-1, \sqrt{R^2-1}]$.*
- *If $R = \sqrt{2}$, then $\varrho > \sqrt{2}-1$ adds no new shape and hence the shape space* (2.1) *is in one-to-one correspondence with*

$$\left\{ i_\varrho(T_{\sqrt{2}}) : \varrho \in [0, \sqrt{2}-1) \right\}.$$

Proof. Recall the two expressions in Lemma 2.3 for $\lambda = r_1/r_2$ in the two intervals of ϱ. It is easy to check that both

$$\lambda_1 : [0, R-1) \to [1, \infty), \quad \lambda_1(\varrho) = \frac{(\varrho + R)^2 - 1}{(\varrho - R)^2 - 1}$$

and

$$\lambda_2 : \big(R-1, \sqrt{R^2-1}\big] \to [1, \infty), \quad \lambda_2(\varrho) = \frac{(R-1)[(R+1)^2 - \varrho^2]}{(R+1)[\varrho^2 - (R-1)^2]}$$

are bijections: simply check that λ_1 is monotonic increasing from 1 to ∞, and λ_2 is monotonic decreasing from ∞ to 1. As the $r_1 : r_2$ ratio of $i_\varrho(T_R)$ is distinct for different $\varrho \in [0, R-1)$, the first statement of the theorem is true. Likewise, $i_\varrho(T_R)$ is also distinct for each $\varrho \in (R-1, \sqrt{R^2-1}]$.

To show the statement in the first bullet, it remains to argue that for $\varrho_1 \in [0, R-1)$ and $\varrho_2 \in (R-1, \sqrt{R^2-1}]$, $i_{\varrho_1}(T_R) \neq i_{\varrho_2}(T_R)$. There are two cases:

(1) If $\lambda_1(\varrho_1) \neq \lambda_2(\varrho_2)$, then $i_{\varrho_1}(T_R) \neq i_{\varrho_2}(T_R)$.
(2) If $\lambda_1(\varrho_1) = \lambda_2(\varrho_2)$, then, by the expressions of the $r_2 : d$ ratio in Lemma 2.3, the $r_2 : d$ ratios of $i_{\varrho_1}(T_R)$ and $i_{\varrho_2}(T_R)$ are different exactly when $R^2 \neq \frac{R^2}{R^2-1}$. But
$$R^2 = \frac{R^2}{R^2-1} \iff R = \sqrt{2}.$$
So we also have $i_{\varrho_1}(T_R) \neq i_{\varrho_2}(T_R)$ in this case.

This argument proves the statement under the second bullet as well. ∎

The next two results characterize the bigger shape space (2.2); they are inspiring for us but technically we do not need them for this article. We omit the detailed proofs, which follow the same line of arguments as in that of Theorem 2.4.

Lemma 2.5. *For any $R \in (1, \infty)$, $\varrho \in [0, \sqrt{R^2-1}]$,*

$$i_\varrho(T_R) = i_{\varrho'}(T_{R'}) \quad \text{where} \quad (R', \varrho') = \frac{1}{\sqrt{R^2-1}}\Big(R, \frac{\sqrt{R^2-1} - \varrho}{\sqrt{R^2-1} + \varrho}\Big). \tag{2.16}$$

Theorem 2.6. *Let*

$$C_R := \begin{cases} [0, \sqrt{R^2-1}] \backslash \{R-1\} & \text{if } R \in (1, \sqrt{2}) \\ [0, \sqrt{2}-1) & \text{if } R = \sqrt{2} \end{cases}, \quad C := \bigcup_{R \in (1, \sqrt{2}]} \{(R, \varrho) : \varrho \in C_R\}.$$

Distinct elements in C correspond to distinct $i_\varrho(T_R)$ and the shape space (2.2) *is in one-to-one correspondence with $\big\{i_\varrho(T_R) : (R, \varrho) \in C\big\}$.*

3. Step II: Rounding by sphere inversion

Theorem 3.1. *If S is a compact regular surface (with or without boundary) in $\mathbb{R}^3$ and $p \in S$, then*

$$\text{Area}(i_q(S)) \sim \frac{\pi}{|p-q|^2}, \quad q \to p, \quad \overline{pq} \perp T_pS. \tag{3.1}$$

If S is also closed and orientable (so S and $i_q(S)$ have enclosed volumes), then

$$\text{Volume}(i_q(S)) \sim \frac{\pi}{6|p-q|^3}, \quad q \to p, \quad \overline{pq} \perp T_pS, \tag{3.2}$$

and (consequently)

$$v(i_q(S)) = \frac{\text{Volume}(i_q(S))}{(4\pi/3)\,(\text{Area}(i_q(S))/(4\pi))^{3/2}} \to 1, \quad q \to p, \quad \overline{pq} \perp T_pS. \tag{3.3}$$

Proof. Without loss of generality assume $p = (0,0,0)$ and T_pS is the x-y plane, and let ε be a small scalar representing the point $q = (0,0,\varepsilon)$ approaching the surface orthogonally at the origin. So the surface near p can be written as the graph of a smooth function $h(x,y)$, where $x^2+y^2 < R^2$ for some $R > 0$ and h has a vanishing linear approximation at the origin, i.e. $h(0,0) = 0 = \frac{\partial h}{\partial x}(0,0) = \frac{\partial h}{\partial y}(0,0)$, and so

$$h(x,y) = O(x^2+y^2), \quad |\nabla h(x,y)| = O(\sqrt{x^2+y^2}), \quad (x,y) \to (0,0). \tag{3.4}$$

Write $S_R := \{(x,y,h(x,y)) : x^2+y^2 < R^2\}$. By continuity, the area of $i_{(0,0,\varepsilon)}(S\backslash S_R)$ approaches that of $i_{(0,0,0)}(S\backslash S_R)$ as $\varepsilon \to 0$ and hence stays bounded for small ε. So it suffices to prove (3.1) with S replaced by S_R.

The conformal factor of $i_{\mathbf{a}}$ is $\lambda^2(\mathbf{a},\mathbf{x}) = 1/\|\mathbf{x}-\mathbf{a}\|^4$, i.e. $\langle di_{\mathbf{a}}|_{\mathbf{x}}v, di_{\mathbf{a}}|_{\mathbf{x}}w\rangle = \lambda^2(\mathbf{a},\mathbf{x})\langle v,w\rangle$. Therefore,

$$\begin{aligned}\text{Area}(i_{(0,0,\varepsilon)}(S_R)) &= \iint_{x^2+y^2<R^2} \frac{\sqrt{1+|\nabla h(x,y)|^2}}{[x^2+y^2+(h(x,y)-\varepsilon)^2]^2}\,dxdy \\ &= \int_0^{2\pi}\left[\int_0^R \frac{\sqrt{1+|\nabla h(re^{i\theta})|^2}}{[r^2+(\varepsilon-h(re^{i\theta}))^2]^2}\,rdr\right]d\theta.\end{aligned} \tag{3.5}$$

Let $r_*(\varepsilon) = |\varepsilon|^\alpha$ for any $\alpha \in (1/2,1)$ (e.g. $\alpha = 2/3$ would do.) As such,

$$\text{(i) } |\varepsilon| = o(r_*(\varepsilon)) \quad \text{and} \quad \text{(ii) } r_*(\varepsilon) = o(|\varepsilon|^{1/2}), \quad \text{as } \varepsilon \to 0. \tag{3.6}$$

We then split the inner integral in (3.5) into $\int_0^{r_*(\varepsilon)} + \int_{r_*(\varepsilon)}^R$; define

$$\begin{aligned}J(\varepsilon) &:= \int_0^{2\pi}\int_0^{r_*(\varepsilon)} \frac{\sqrt{1+|\nabla h(re^{i\theta})|^2}}{[r^2+(\varepsilon-h(re^{i\theta}))^2]^2}\,rdrd\theta, \\ K(\varepsilon) &:= \int_0^{2\pi}\int_{r_*(\varepsilon)}^{K} \frac{\sqrt{1+|\nabla h(re^{i\theta})|^2}}{[r^2+(\varepsilon-h(re^{i\theta}))^2]^2}\,rdrd\theta.\end{aligned}$$

We shall prove (3.1) by showing that the former integral is asymptotically equivalent to $\varepsilon^{-2}/2$ and the latter grows slower than ε^{-2}.

For $J(\varepsilon)$, we compare it with the special case when $h \equiv 0$. By (3.4), there exists a constant $C > 0$, independent of r and θ, such that

$$|\nabla h(re^{i\theta})|^2,\ |h(re^{i\theta})| \leqslant Cr^2.$$

For $r \in [0, r_*(\varepsilon)]$, $r^2 \leqslant r_*(\varepsilon)^2 = o(|\varepsilon|)$ by (3.6)(ii), so $\varepsilon - h(re^{i\theta}) \sim \varepsilon$. Also, $1+|\nabla h(re^{i\theta})|^2 \sim 1$. From this it is easy to see that

$$J(\varepsilon) \sim \int_0^{2\pi}\int_0^{r_*(\varepsilon)} \frac{r}{[r^2+\varepsilon^2]^2}\,drd\theta. \tag{3.7}$$

The right-hand side is $J(\varepsilon)$ in the case of $h \equiv 0$, whose asymptotic can be easily determined:

$$\begin{aligned}&\int_0^{2\pi}\int_0^{r_*(\varepsilon)} \frac{r}{[r^2+\varepsilon^2]^2}\,drd\theta \\ &\quad = \frac{2\pi}{\varepsilon^2}\int_0^{r_*(\varepsilon)/\varepsilon} \frac{s\,ds}{(1+s^2)^2} = \frac{2\pi}{\varepsilon^2}\left[\frac{1}{2} - \frac{1}{2(1+(r_*(\varepsilon)/\varepsilon)^2)}\right] \sim \frac{\pi}{\varepsilon^2}, \quad \varepsilon \to 0.\end{aligned} \tag{3.8}$$

In the last step above, we used (3.6)(i).

For $K(\varepsilon)$, note that ∇h is bounded on a compact set, so

$$\begin{aligned} K(\varepsilon) &= \int_0^{2\pi} \int_{r_*(\varepsilon)}^{R} \frac{\sqrt{1+|\nabla h(re^{i\theta})|^2}}{[r^2+(\varepsilon - h(re^{i\theta}))^2]^2}\, r dr d\theta \\ &\leqslant 2\pi \int_{r_*(\varepsilon)}^{R} \frac{C}{[r^2]^2}\, r dr \\ &\leqslant 2\pi C \int_{r_*(\varepsilon)}^{\infty} r^{-3} dr = \pi C r_*(\varepsilon)^{-2} = o(\varepsilon^{-2}). \end{aligned}$$

In the last step above, we again used (3.6)(i).

We have completed the proof of (3.1).

Let B be a ball whose boundary is tangent to S at p and lies inside of S, so $\text{Volume}(B) \leqslant \text{Volume}(S)$ and also

$$\text{Volume}(i_q(B)) \leqslant \text{Volume}(i_q(S)).$$

As before, write $|p-q| = \varepsilon$. Since $i_q(B)$ is a ball with diameter $\sim 1/\varepsilon$, $\text{Volume}(i_q(B)) \sim \frac{4\pi}{3}\left(\frac{1}{2\varepsilon}\right)^3 = \frac{\pi}{6\varepsilon^3}$, $\varepsilon \to 0$. So $\text{Volume}(i_q(S))$ grows at least as fast as $\pi/(6\varepsilon^3)$. By the first part of the theorem and the isoperimetric inequality, $\text{Volume}(i_q(S))$ cannot grow faster than $\pi/(6\varepsilon^3)$, and (3.2) is proved. ∎

4. Step III: Reduction to P-recurrence

In this section we express by P-recurrences the surface area and enclosed volume of $i_{\mathbf{a}}(T_{\sqrt{2}})$, where $\mathbf{a} = [a,0,0]^T$, $a \in [0, \sqrt{2}-1)$, which are the same as those of $\text{SCT}_{\mathbf{a}}(T_{\sqrt{2}})$, where $\text{SCT}_{\mathbf{a}} := i \circ t_{\mathbf{a}} \circ i$, $t_{\mathbf{a}}$ is translation by $\mathbf{a}$. (Recall $i(T_{\sqrt{2}}) = T_{\sqrt{2}}$.) From these, an associated P-recurrence related to the isoperimetric ratio of $i_{\mathbf{a}}(T_{\sqrt{2}})$ will also be derived.

4.1. **Area and volume integrals.** The conformal factor of a special conformal transformation $\text{SCT}_{\mathbf{a}} := i \circ t_{\mathbf{a}} \circ i$ is

$$\lambda^2(\mathbf{a}, \mathbf{x}) = \frac{1}{(1+2\langle \mathbf{a}, \mathbf{x}\rangle + \langle \mathbf{a}, \mathbf{a}\rangle\langle \mathbf{x}, \mathbf{x}\rangle)^2},$$

i.e. $\langle d\text{SCT}_{\mathbf{a}}|_{\mathbf{x}} v, d\text{SCT}_{\mathbf{a}}|_{\mathbf{x}} w\rangle = \lambda^2(\mathbf{a},\mathbf{x})\langle v, w\rangle$. So the area and enclosed volume of $\text{SCT}_{[a,0,0]}(T_{\sqrt{2}})$ are given by

$$\begin{aligned} A(a) &= \int_0^{2\pi} \int_0^{2\pi} Q(a;\mathbf{x})^{-2}\, d\text{Area}(u,v), \\ V(a) &= \int_0^1 \int_0^{2\pi} \int_0^{2\pi} Q(a;\mathbf{x})^{-3}\, d\text{Vol}(u,v,r), \end{aligned}$$

where

$$Q(a;\mathbf{x}) := \frac{1}{\lambda([a,0,0]^T, \mathbf{x})} = 1 + 2\mathbf{x}_1 a + \|\mathbf{x}\|^2 a^2,$$

$$\mathbf{x}(u,v,r) = \left[\left(\sqrt{2}+r\sin(v)\right)\cos(u),\ \left(\sqrt{2}+r\sin(v)\right)\sin(u),\ r\cos(v)\right], \quad u, v \in [0, 2\pi],\quad r \in [0,1],$$

$$d\text{Area}(u,v) = (\sqrt{2}+\sin(v))\, du\, dv, \quad d\text{Vol}(u,v,r) = r(\sqrt{2}+r\sin(v))\, du\, dv\, dr.$$

Notice also that

$$\langle \mathbf{x}, \mathbf{x}\rangle = \|\mathbf{x}\|^2 = 2 + r^2 + 2\sqrt{2} r \sin(v).$$

4.2. **Holomorphic extension.** The integral definitions of A and V above extend from the interval $[0, \sqrt{2}-1)$ to a holomorphic function on the open disk

$$D := \{z \in \mathbb{C} : |z| < \sqrt{2}-1\}.$$

To see this, note that the roots of $Q(z; \mathbf{x})$, viewed as a quadratic polynomial in z, can be expressed as

$$\frac{-\mathbf{x}_1 \pm i\sqrt{\mathbf{x}_2^2 + \mathbf{x}_3^2}}{\|\mathbf{x}\|^2},$$

so their moduli are both $1/\|\mathbf{x}\|$. But $\mathbf{x}$ is a point in the boundary or interior of the solid torus T, so $\|\mathbf{x}\| \in [\sqrt{2}-1, \sqrt{2}+1]$, which is equivalent to $1/\|\mathbf{x}\| \in [\sqrt{2}-1, \sqrt{2}+1]$. This means

$$Q(z; \mathbf{x}) \neq 0, \quad \forall\, z \in D, \quad \mathbf{x} \in T.$$

Therefore $Q(z; \mathbf{x})^{-L}$, $L = 2$ or 3, is holomorphic in the first argument and continuous in the second. A standard argument in complex analysis shows that A and V, defined based on the integrals in (4.1), extend to holomorphic functions on D.

So from now on, we write $A(z)$ and $V(z)$ instead of $A(a)$ and $V(a)$.

4.3. **Power series at $z = 0$.** Since A and V are even functions, the odd power Taylor coefficients at $z = 0$ all vanish. Denote by a_j and v_j the coefficients of z^{2j} in the expansions of $A(z)$ and $V(z)$ at $z = 0$, respectively. An observation here is that

$$\begin{aligned} \frac{d^n A}{dz^n}(0) &= \iint_{\partial T} \frac{d^n}{dz^n} Q(z; \mathbf{x}(u,v,1))^{-2}\Big|_{z=0} d\mathrm{Area}(u,v) \\ \frac{d^n V}{dz^n}(0) &= \iiint_{T} \frac{d^n}{dz^n} Q(z; \mathbf{x}(u,v,r))^{-3}\Big|_{z=0} d\mathrm{Vol}(u,v,r), \end{aligned} \tag{4.1}$$

and, thanks to the evaluation at $z = 0$, the integrands above are *polynomials* in $\mathbf{x}_1$ and $\|\mathbf{x}\|^2$, hence are *trigonometric polynomials* in (u, v).

Using either (4.1) or the generalized binomial theorem to expand $Q(z; \mathbf{x})^{-L}$ into a power series of z, i.e.

$$Q(z; \mathbf{x})^{-L} = \sum_{n=0}^{\infty} \binom{n+L-1}{n} (-1)^n (2\mathbf{x}_1 z + \|\mathbf{x}\|^2 z^2)^n,$$

together with the identity (of Wallis' integrals):

$$\int_0^{2\pi} \cos^n(v)\, dv = \int_0^{2\pi} \sin^n(v)\, dv = \begin{cases} \frac{2\pi}{2^n}\binom{n}{n/2}, & n \text{ even} \\ 0, & n \text{ odd} \end{cases},$$

we have

$$\begin{aligned}
a_j &= \sum_{\ell=0}^{j}(-1)^{j-\ell}\,(j+\ell+1)\binom{j+\ell}{j-\ell} \\
&\qquad\qquad \times \int_0^{2\pi}\int_0^{2\pi}(2\mathbf{x}_1(u,v,1))^{2\ell}\|\mathbf{x}(u,v,1)\|^{2(j-\ell)}d\mathrm{Area}(u,v) \\
&= \sum_{\ell=0}^{j}(-1)^{j-\ell}\,(j+\ell+1)\binom{j+\ell}{j-\ell}\,4^{\ell} \\
&\quad \times \underbrace{\int_0^{2\pi}\cos^{2\ell}(u)\,du}_{=2\pi\binom{2\ell}{\ell}/4^{\ell}} \quad \underbrace{\int_0^{2\pi}(\sqrt{2}+\sin(v))^{2\ell+1}(3+2\sqrt{2}\sin(v))^{j-\ell}dv.}_{=\sum_{p=0}^{2\ell+1}\sum_{q=0}^{j-\ell}\binom{2\ell+1}{p}\sqrt{2}^{2\ell+1-p}\binom{j-\ell}{q}3^{j-\ell-q}(2\sqrt{2})^q\int_0^{2\pi}\sin^{p+q}(v)\,dv}
\end{aligned}$$

So,

$$\begin{aligned}
a_j &= \sqrt{2}\pi^2\sum_{\ell=0}^{j}(-1)^{j-\ell}\,(j+\ell+1)\binom{j+\ell}{j-\ell,\ell,\ell}\,\alpha_{\ell,j}, \\
\alpha_{\ell,j} &= 2^{\ell+2}3^{j-\ell}\underbrace{\sum_{p=0}^{2\ell+1}\sum_{q=0}^{j-\ell}}_{p+q=\text{even}}\binom{2\ell+1}{p}\binom{j-\ell}{q}\binom{p+q}{(p+q)/2}2^{(q-3p)/2}3^{-q}.
\end{aligned} \tag{4.2}$$

Similarly,

$$\begin{aligned}
v_j &= \sum_{\ell=0}^{j}(-1)^{j-\ell}\,\frac{(j+\ell+1)(j+\ell+2)}{2}\binom{j+\ell}{j-\ell} \\
&\qquad\qquad \times \int_0^1\int_0^{2\pi}\int_0^{2\pi}(2\mathbf{x}_1(u,v,r))^{2\ell}\|\mathbf{x}(u,v,r)\|^{2(j-\ell)}d\mathrm{Vol}(u,v,r) \\
&= \sum_{\ell=0}^{j}(-1)^{j-\ell}\,\frac{(j+\ell+1)(j+\ell+2)}{2}\binom{j+\ell}{j-\ell}\,4^{\ell}\underbrace{\int_0^{2\pi}\cos^{2\ell}(u)\,du}_{=2\pi\binom{2\ell}{\ell}/4^{\ell}} \\
&\quad \times \qquad \underbrace{\int_0^1\int_0^{2\pi}r(\sqrt{2}+r\sin(v))^{2\ell+1}(2+r^2+2\sqrt{2}r\sin(v))^{j-\ell}dvdr.}_{\sum_{p=0}^{2\ell+1}\sum_{q=0}^{j-\ell}\binom{2\ell+1}{p}\sqrt{2}^{2\ell+1-p}\binom{j-\ell}{q}(2\sqrt{2})^q\int_0^{2\pi}\sin^{p+q}(v)\,dv\int_0^1 r^{p+q+1}(2+r^2)^{j-\ell-q}\,dr}
\end{aligned}$$

So,

$$\begin{aligned}
v_j &= \sqrt{2}\pi^2\sum_{\ell=0}^{j}(-1)^{j-\ell}\,(j+\ell+1)(j+\ell+2)\binom{j+\ell}{j-\ell,\ell,\ell}\,\nu_{\ell,j}, \\
\nu_{\ell,j} &= 2^{\ell+1}\underbrace{\sum_{p=0}^{2\ell+1}\sum_{q=0}^{j-\ell}}_{p+q=\text{even}}\binom{2\ell+1}{p}\binom{j-\ell}{q}\binom{p+q}{(p+q)/2}2^{(q-3p)/2}\eta_{p,q,\ell,j}, \\
\eta_{p,q,\ell,j} &= \int_0^1 r^{p+q+1}(2+r^2)^{j-\ell-q}\,dr = \sum_k^{j-\ell-q}\binom{j-\ell-q}{k}\frac{2^{j-\ell-q-k}}{2k+p+q+2}.
\end{aligned} \tag{4.3}$$

And we have the following power series:

$$\begin{aligned}\frac{1}{\sqrt{2}\pi^2}A(z) &= 4 + 52\,z^2 + 477\,z^4 + 3809\,z^6 + \frac{451625}{16}\,z^8 + \cdots\\ \frac{1}{\sqrt{2}\pi^2}V(z) &= 2 + 48\,z^2 + \frac{1269}{2}\,z^4 + 6600\,z^6 + \frac{1928025}{32}\,z^8 + \cdots\end{aligned}$$

By the expressions (4.2)-(4.3), $\frac{1}{\sqrt{2}\pi^2}a_n$, $\frac{1}{\sqrt{2}\pi^2}v_n$ are rational.

4.4. **Isoperimetric ratio.** To show that the isoperimetric ratio of $\mathrm{SCT}_{[a,0,0]}(T_{\sqrt{2}})$ is monotonic increasing in $a \in [0, \sqrt{2}-1)$, it suffices to show

$$\Delta(a) := \frac{d}{da}\ln\frac{V(a)^2}{A(a)^3} = 2\frac{V'(a)}{V(a)} - 3\frac{A'(a)}{A(a)} > 0, \quad \text{or} \quad 2V'(a)A(a) - 3V(a)A'(a) > 0.$$

It happens that $\Delta(a)$ is proportional to the distance between the area and volume centers of the cyclide $\mathrm{SCT}_{[a,0,0]}(T_{\sqrt{2}})$. Precisely, $\Delta(a) = 12\big[\mathbf{x}^A(a) - \mathbf{x}^V(a)\big]$ where $\mathbf{x}^A(a)$ and $\mathbf{x}^V(a)$ are the first coordinates of the area and volume centers of $\mathrm{SCT}_{[a,0,0]}(T_{\sqrt{2}})$, respectively.[5] This follows from the observation that $(\mathrm{SCT}_{[a,0,0]} \circ \mathbf{x})_1 = \frac{1}{2}Q'(a;\mathbf{x})/Q(a;\mathbf{x})$.

By the Taylor expansions of $A(a)$ and $V(a)$, we have

$$\begin{aligned}(4.4)\quad & 2V'(a)A(a) - 3V(a)A'(a)\\ &= 2\sum_{k=0}^{\infty}\underbrace{\left[\begin{array}{l}2(v_1a_k + 2v_2a_{k-1} + \cdots + (k+1)v_{k+1}a_0)\\ \qquad -3(a_1v_k + 2a_2v_{k-1} + \cdots + (k+1)a_{k+1}v_0)\end{array}\right]}_{=:d_k} a^{2k+1}\\ &= 4\pi^4\Big(72\,a + 1932\,a^3 + 31248\,a^5 + \frac{790101}{2}\,a^7 + \frac{17208645}{4}\,a^9 + \cdots\Big).\end{aligned}$$

4.5. **P-recurrences.** The combinatorial expressions (4.2) and (4.3), together with the closure properties of holonomic sequences [7, 14, 17], show that $(a_n)_{n\geqslant 0}$ and $(v_n)_{n\geqslant 0}$ are P-recursive, i.e. they satisfy linear recurrences with polynomial coefficients. Equivalently, their generating functions, namely $\bar{A}(z) = \sum_{n\geqslant 0} a_n z^n$, $\bar{V}(z) = \sum_{n\geqslant 0} v_n z^n$, are holonomic or D-finite, i.e. they satisfy linear differential equations with polynomial coefficients. The generating functions of $(a_n)_{n\geqslant 0}$ and $(v_n)_{n\geqslant 0}$ are related to the original area and volume functions $A(z)$ and $V(z)$ simply by $A(z) = \bar{A}(z^2)$ and $V(z) = \bar{V}(z^2)$. The generating function of the sequence $(d_k)_{k\geqslant 0}$, defined by (4.4), is given by

$$\bar{D}(z) := \sum_{n=0}^{\infty} d_n z^n = 2\bar{V}'(z)\bar{A}(z) - 3\bar{V}(z)\bar{A}'(z).$$

Since holonomic functions are closed under Hadamard product (hence differentiation), product, and linear combination, $(d_n)_{n\geqslant 0}$ is also holonomic.

[5]According to this formula, Theorem 1.1 is proved if one establishes that $\mathbf{x}^A(a) \neq \mathbf{x}^V(a)$ for all $a \in (0, \sqrt{2}-1)$. At one point, the first author presented an incomplete argument to R. Kusner based on this approach. He thanks Kusner for helping him to see the flaw in his argument.

Proposition 4.1. *The P-recurrences of $(a_n)_{n\geqslant 0}$, $(v_n)_{n\geqslant 0}$ and $(d_n)_{n\geqslant 0}$ are given by*

(4.5)

$$\sum_{i=0}^{3} p_i(n)a_{n+i} = 0, \ \ where \ \begin{bmatrix} p_0(n) \\ p_1(n) \\ p_2(n) \\ p_3(n) \end{bmatrix} = \begin{bmatrix} -84 & -136 & -81 & -21 & -2 \\ 399 & 730 & 484 & 137 & 14 \\ -474 & -835 & -529 & -143 & -14 \\ 54 & 99 & 66 & 19 & 2 \end{bmatrix} \begin{bmatrix} 1 \\ n \\ n^2 \\ n^3 \\ n^4 \end{bmatrix}$$

(4.6)

$$\sum_{i=0}^{3} q_i(n)v_{n+i} = 0, \ \ where \ \begin{bmatrix} q_0(n) \\ q_1(n) \\ q_2(n) \\ q_3(n) \end{bmatrix} = \begin{bmatrix} -252 & -303 & -136 & -27 & -2 \\ 960 & 1384 & 730 & 167 & 14 \\ -1008 & -1436 & -748 & -169 & -14 \\ 90 & 141 & 82 & 21 & 2 \end{bmatrix} \begin{bmatrix} 1 \\ n \\ n^2 \\ n^3 \\ n^4 \end{bmatrix}$$

(4.7)

$$\sum_{i=0}^{7} r_i(n)d_{n+i} = 0, \ \ where \ [r_0(n), r_1(n), \dots, r_7(n)]^T = M[1, n, n^2, \dots, n^7]^T,$$

$$M = \begin{bmatrix} -\frac{1630207404}{1529} & -\frac{3176073675}{3058} & -\frac{660587685}{1529} & -\frac{1216898711}{12232} & -\frac{167529251}{12232} & -\frac{626799}{556} & -\frac{7141}{139} & -1 \\ \frac{18219511026}{1529} & \frac{6798395835}{556} & \frac{16328931207}{3058} & \frac{15735207287}{12232} & \frac{2258693435}{12232} & \frac{8782801}{556} & \frac{103675}{139} & 15 \\ -\frac{80949464718}{1529} & -\frac{338705850511}{6116} & -\frac{150907466733}{6116} & -\frac{74228837833}{12232} & -\frac{10882115811}{12232} & -\frac{43223443}{556} & -\frac{521157}{139} & -77 \\ \frac{347623458975}{3058} & \frac{32991350565}{278} & \frac{322759355227}{6116} & \frac{158457515673}{12232} & \frac{23184921987}{12232} & \frac{91902509}{556} & \frac{1105723}{139} & 163 \\ -\frac{368052969807}{3058} & -\frac{190572156372}{1529} & -\frac{168114763631}{3058} & -\frac{163720428321}{12232} & -\frac{23758375953}{12232} & -\frac{93404429}{556} & -\frac{1114663}{139} & -163 \\ \frac{177327816597}{3058} & \frac{366011927673}{6116} & \frac{40230202855}{1529} & \frac{78121412337}{12232} & \frac{11304865929}{12232} & \frac{44328883}{556} & \frac{527737}{139} & 77 \\ -\frac{29809040325}{3058} & -\frac{62775138251}{6116} & -\frac{28175845633}{6116} & -\frac{13970430847}{12232} & -\frac{2065443305}{12232} & -\frac{8275441}{556} & -\frac{100655}{139} & -15 \\ \frac{818331696}{1529} & \frac{880217988}{1529} & \frac{1617383067}{6116} & \frac{822460415}{12232} & \frac{124982969}{12232} & \frac{515919}{556} & \frac{6481}{139} & 1 \end{bmatrix}.$$

Moreover, these are the only P-recurrences with the corresponding order (r) *and degree* (d) *for the three sequences. (E.g.,* (4.5) *is the only P-recurrence with* $(r, d) = (3, 4)$ *satisfied by the sequence* (a_n)*.)*

As one may expect from the appearance of the result, the proof is computer-assisted. The first part of the proposition, namely, the sequences defined by (4.2)–(4.4) satisfy the P-recurrences (4.5)–(4.7), can be established by a refinement of Zeilberger's *creative telescoping method* [17] due to Koutschan [8] (implemented in his Mathematica package `HolonomicFunctions`.) We can check the second part of the claim in an elementary fashion. Assume that we have established that (a_n) follows a P-reccurence of order $r = 3$ and degree $d = 4$, then the $(d+1)(r+1) = 20$ coefficients in the polynomials satisfy, for every index n, a homogeneous linear equation with rational coefficients determined by the terms $a_n, a_{n+1}, a_{n+2}, a_{n+3}$. Using the first $N + 4$ terms of the sequence a_n with any $N \geqslant 20$, easily computable by (4.2), we can set up a homogeneous linear system that must be satisfied by the 20 coefficients. Using a symbolic linear solver to explicitly work out a basis of the null space of the rational $N \times 20$ coefficient matrix, and seeing that the basis consists of one vector in $\mathbb{R}^{20}$ with a certain $N \geqslant 20$, would not only prove the claimed uniqueness (up to a scaling factor), but also reproduce the P-recurrence in

(4.5). This method is called 'guessing' in [7], as it can be used to guess (with high confidence) what the P-recurrence might be when used with a big enough N.

Using asymptotic techniques [5, 6, 12, 15] of holonomic functions, aided by rigorous interval arithmetic computation, it can be shown that $d_n \sim c \cdot \big(\sqrt{2}+1\big)^{2n} n^3 \ln(n)$, $c > 8$. This is more than enough for proving that d_n is eventually positive, but is insufficient for verifying full positivity. Melczer and Mezzarobba's proof of positivity [13] is based on streamlining existing complex analytic techniques [5, 12] in order to bound the error in the asympototic approximation above.

Acknowledgments

We thank Robert Kusner for bringing to our attention the uniqueness problem and his earlier involvement of this project. We are grateful to Manuel Kauers, Stephen Melczer and Pierre Lairez for sharing their expertise in P-recurrences.

We thank I. Pinelis for the help in analyzing the asymptotic of the area integral (3.5); see `https://mathoverflow.net/questions/353648/asymptotic-of-an-area-integral`.

References

[1] David E. Blair, *Inversion theory and conformal mapping*, Student Mathematical Library, vol. 9, American Mathematical Society, Providence, RI, 2000, DOI 10.1090/stml/009. MR1779832

[2] Wolfgang Boehm, *On cyclides in geometric modeling*, Comput. Aided Geom. Design **7** (1990), no. 1-4, 243–255, DOI 10.1016/0167-8396(90)90034-O. Curves and surfaces in CAGD '89 (Oberwolfach, 1989). MR1074612

[3] V. Chandru, D. Dutta, and C. M. Hoffmann, *On the geometry of Dupin cyclides*, Vis. Comput., **5** (1989), no. 5, 277–290.

[4] Jingmin Chen, Thomas Yu, Patrick Brogan, Robert Kusner, Yilin Yang, and Andrew Zigerelli, *Numerical methods for biomembranes: conforming subdivision methods versus non-conforming PL methods*, Math. Comp. **90** (2021), no. 328, 471–516, DOI 10.1090/mcom/3584. MR4194152

[5] Philippe Flajolet and Robert Sedgewick, *Analytic combinatorics*, Cambridge University Press, Cambridge, 2009, DOI 10.1017/CBO9780511801655. MR2483235

[6] M. Kauers, *A mathematica package for computing asymptotic expansions of solutions of P-finite recurrence equations*, Technical report, RISC-Linz, 2011. Tech. Rep. 11-04.

[7] Manuel Kauers and Peter Paule, *The concrete tetrahedron*, Texts and Monographs in Symbolic Computation, SpringerWienNewYork, Vienna, 2011. Symbolic sums, recurrence equations, generating functions, asymptotic estimates, DOI 10.1007/978-3-7091-0445-3. MR2768529

[8] Christoph Koutschan, *A fast approach to creative telescoping*, Math. Comput. Sci. **4** (2010), no. 2-3, 259–266, DOI 10.1007/s11786-010-0055-0. MR2775992

[9] R. Kusner, A. Mondino, and F. Schulze, *Willmore bending energy on the space of surfaces*, EMISSARY, Mathematical Sciences Research Institute, Spring 2016. Available at `http://www.msri.org/system/cms/files/204/files/original/Emissary-2016-Spring-Web.pdf`.

[10] Fernando C. Marques and André Neves, *Min-max theory and the Willmore conjecture*, Ann. of Math. (2) **179** (2014), no. 2, 683–782, DOI 10.4007/annals.2014.179.2.6. MR3152944

[11] J. C. Maxwell, *On the cyclide*, Quart. J. Pure Appl. Math. **9** (1868), 111–126.

[12] Stephen Melczer, Marni Mishna, and Robin Pemantle, *Combinatorial adventures in analysis, algebra, and topology*, Notices Amer. Math. Soc. **67** (2020), no. 2, 262–265. MR3971646

[13] S. Melczer and M. Mezzarobba, *Sequence positivity through numeric analytic continuation: Uniqueness of the Canham model for biomembranes*, submitted to J. Comb. Theory, November 2020.

[14] Richard P. Stanley, *Enumerative combinatorics. Vol. 2*, Cambridge Studies in Advanced Mathematics, vol. 62, Cambridge University Press, Cambridge, 1999. With a foreword by Gian-Carlo Rota and appendix 1 by Sergey Fomin, DOI 10.1017/CBO9780511609589. MR1676282

[15] Jet Wimp and Doron Zeilberger, *Resurrecting the asymptotics of linear recurrences*, J. Math. Anal. Appl. **111** (1985), no. 1, 162–176, DOI 10.1016/0022-247X(85)90209-4. MR808671

[16] T. P.-Y. Yu and J. Chen, *On the uniqueness of Clifford torus with prescribed isoperimetric ratio*, March 2020, Available at `https://www.math.drexel.edu/~tyu/Papers/Uniqueness.pdf`.

[17] Doron Zeilberger, *A holonomic systems approach to special functions identities*, J. Comput. Appl. Math. **32** (1990), no. 3, 321–368, DOI 10.1016/0377-0427(90)90042-X. MR1090884

Department of Mathematics, Drexel University, Philadelphia, Pennsylvania 19104
Email address: yut@drexel.edu

Citigroup Global Markets Inc., 390 Greenwich Street, New York, New York 10013
Email address: jingmchen@gmail.com